# A Benchmark set

| PDB-id | Description | Length | Topology | Exploration radius | Execution time (s) | Avg. min $RMSD_{NMR}$ |
|---|---|---|---|---|---|---|
| 2Y95 | AUCG tetraloop human Xist A-repeat | 15 | | 1.3 | 32 | 0.4 |
| 1JU7 | SLBP binding site | 17 | | 2.2 | 234 | 0.7 |
| 2KRY | Mitochondrial tRNA-MET ASL from human | 17 | | 2.6 | 29 | 0.8 |
| 2L6I | Coronoviral stemloop 2 | 17 | | 0.9 | 114 | 0.3 |
| 2LP9 | Pseudo-triloop from BMV | 17 | | 1.8 | 37 | 0.8 |
| 1LUU | ASL of yeast tRNA-PHE | 18 | | 1.4 | 176 | 0.4 |
| 2JSG | Anticodon of E.coli TRNA-VAL3 | 18 | | 1.1 | 35 | 0.4 |
| 2LAC | ASL of b.subtilis tRNA-TYR | 18 | | 0.7 | 38 | 0.3 |
| 2LBJ | ASL of b.subtilis tRNA-GLY | 18 | | 1.0 | 42 | 0.4 |
| 2LBK | ASL of s.epidermis tRNA-GLY | 18 | | 1.5 | 27 | 0.5 |
| 1Z30 | Stemloop D from BEV | 19 | | 1.3 | 389 | 0.4 |
| 2QH4 | scaRNA 5' term hairpin from human telom. | 19 | | 1.8 | 45 | 0.6 |
| 2O32 | U2 snRNA stem I from human | 20 | | 3.4 | 26 | 1.3 |
| 1BN0 | SL3 hairpin | 21 | | 3.7 | 450 | 0.9 |
| 2M21 | Stem IV loop of Tetrahymena telomerase | 22 | | 2.1 | 113 | 0.8 |
| 4A4R | UAAC tetraloop | 22 | | 3.1 | 68 | 0.8 |
| 1PJY | HIV-1 frameshift inducing stem-loop | 23 | | 3.0 | 539 | 1.0 |
| 2JYM | Stemloop A of HBV HPRE | 23 | | 1.8 | 101 | 0.7 |
| 2K66 | d3' stem of group II intron Sc.ai5γ | 23 | | 1.1 | 91 | 0.3 |
| 1OW9 | Active conf. of VS ribozyme | 24 | | 2.3 | 587 | 0.5 |
| 1S34 | Splice site of Rous sarcoma virus | 24 | | 2.6 | 621 | 1.2 |
| 3PHP | 3' hairpin of TYMV pseudoknot | 24 | | 4.9 | 79 | 1.4 |
| 1LC6 | U6 stem loop | 25 | | 3.6 | 699 | 1.0 |
| 2LK3 | Yeast U2/U2 snRNA complex | 25 | | 1.2 | 75 | 0.5 |
| 2LV0 | Helix-35 stemloop of e.coli 23S rRNA | 25 | | 2.9 | 113 | 0.9 |
| 2QH2 | CR7 term hairpin from human telom. | 25 | | 1.9 | 85 | 0.8 |
| 1M82 | cRNA promoter of influenza A | 26 | | 3.0 | 604 | 1.2 |
| 2L5Z | A730 loop of Neurospora VS ribozyme | 27 | | 1.3 | 307 | 0.5 |
| 2LDL | HIV-1 exon splicing silencer 3 | 28 | | 0.9 | 96 | 0.4 |
| 2LJJ | Subdom. IV-B from CVB-3 IRES | 28 | | 2.7 | 151 | 1.1 |
| 2LQZ | RNA claw of DNA packaging motor b29 | 28 | | 2.1 | 125 | 1.0 |
| 2M4Q | Ribosomela decoding site of e.coli | 28 | | 6.0 | 154 | 1.7 |
| 1KPY | PEMV-1 P1-P2 frameshifting pseudoknot | 29 | P | 2.6 | 691 | 1.4 |
| 1YG3 | ScYLV P1-P2 frameshifting pseudoknot | 29 | P | 2.7 | 687 | 1.2 |
| 2JWV | High affinity anti-NFkB RNA aptamer | 30 | | 3.4 | 156 | 0.9 |
| 2K63 | EBS1 of group II intron Sc.ai5γ | 30 | | 4.1 | 173 | 2.0 |
| 2L8H | HIV-1 TAR bound to probe | 30 | | 1.5 | 112 | 0.5 |
| 1HWQ | VS ribozyme substrate | 31 | | 9.0 | 1020 | 2.6 |
| 1LDZ | Lead-dependent ribozyme | 31 | | 7.8 | 749 | 1.8 |
| 1NA2 | P2B hairpin from human telomerase | 31 | | 2.4 | 755 | 0.9 |
| 1MFY | C4 promoter of influenza A | 32 | | 4.1 | 760 | 1.5 |
| 1XHP | Extendd U6 ISL | 33 | | 0.8 | 615 | 0.3 |
| 2LI4 | Antiterminator from Mg2+ riboswitch | 33 | | 7.7 | 185 | 2.1 |
| 1R2P | D5 from ai5γ group II intron | 35 | | 6.3 | 896 | 2.3 |
| 1R7W | D4 stem-loop B of enterovirus IRES | 35 | | 8.8 | 846 | 2.9 |
| 2JTP | Frameshift-inducing stem-loop in SIV | 35 | | 3.2 | 187 | 1.0 |
| 2L3E | P2a-J2a/b-P2b of human telomerase | 36 | | 3.5 | 478 | 1.1 |
| 1N8X | HIV1 stem loop SL1 | 37 | | 3.4 | 765 | 1.2 |
| 2FDT | Hairpin of eel LINE UnaL2 | 37 | | 1.8 | 165 | 0.8 |
| 2L1V | PreQ1 riboswitch bound to preQ1 | 37 | P | 1.2 | 661 | 0.6 |
| 2LUB | Helix H1 of human HAR1 | 38 | | 2.3 | 167 | 1.0 |
| 1MNX | Loop region of 5S rRNA | 43 | | 2.3 | 996 | 1.1 |
| 1A60 | T and acceptor arm of TYMV | 45 | P/B | 4.9 | 1010 | 2.0 |
| 2L94 | HIV-1 frameshift site bound to inhibitor | 46 | | 2.8 | 168 | 0.9 |
| 1YMO | P2b-P3 p.knot from human telomerase | 48 | P | 2.4 | 1140 | 1.0 |
| 2M8K | Pyr motif triple helix of k.lactis telomerase | 49 | P | 1.9 | 388 | 0.9 |
| 2LU0 | κ-ζ reg. of group II intron Sc.ai5γ | 50 | | 10.0 | 439 | 3.2 |
| 2KZL | GA motif of B. subtilis tyrS T box leader | 56 | | 2.4 | 890 | 1.1 |
| 2LC8 | MLV readthrough pseudoknot | 57 | P | 5.1 | 347 | 2.3 |
| 2M58 | 2'-5' AG1 lariat forming ribozyme | 59 | P/B | 22.9 | 572 | 9.8 |
| | | | | | | |
| Min | | 15 | | 0.7 | 26 | 0.3 |
| Max | | 59 | | 22.9 | 1140 | 9.8 |
| Avg | | 30 | | 3.4 | 372 | 1.2 |

**Table ST1.** Benchmark set details. The 60 RNA molecules represent non-redundant single-chain structures from the BMRB with more than 15 residues. **Topology (column 4)**: A pseudo-knot topology is indicated with a P and bridge-topologies with B. The remaining have tree-like topologies. **Exploration radius (column 5)**: The exploration radius is the largest RMSD between two NMR bundle structures and is used as a cutoff for seed-selection in the sampling procedure. **Avg min RMSD (column 6)** The min $RMSD_{NMR}$ is the smallest C4' RMSD between any member of the KGSrna samples and a particular NMR bundle structure. The average over all NMR bundle structures is reported in column 6.

## B Ensemble backbone torsional distributions

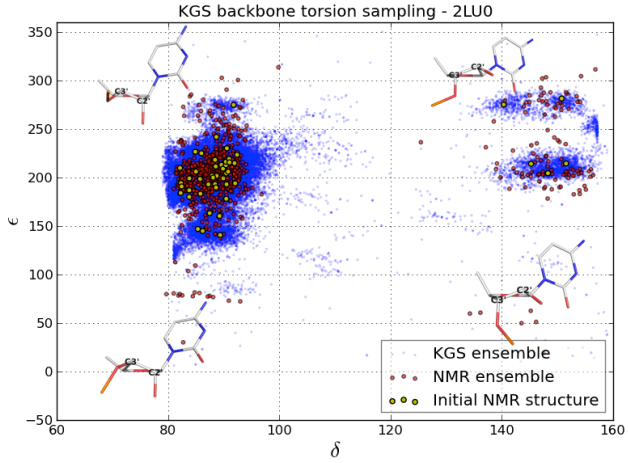


**Fig. S1.** Backbone $\delta - \epsilon$ torsional scatterplot of 1000 KGSrna samples of the S. cerevisiae group II intron (2LU0). The left cluster usually correspond to C3'-endo and the right cluster to C2'-endo ribose conformations. KGSrna extensively samples both regions as well as intermediate ones. Richardson et al. [25] suggests that ribose conformations with $\epsilon < 155^{\circ}$ corresponds to ribose conformations that have wrongly been fitted with C3'-endo conformations while they should have been C2'-endo. Interestingly, very few KGSrna samples lie in the region where $\epsilon < 100^{\circ}$.

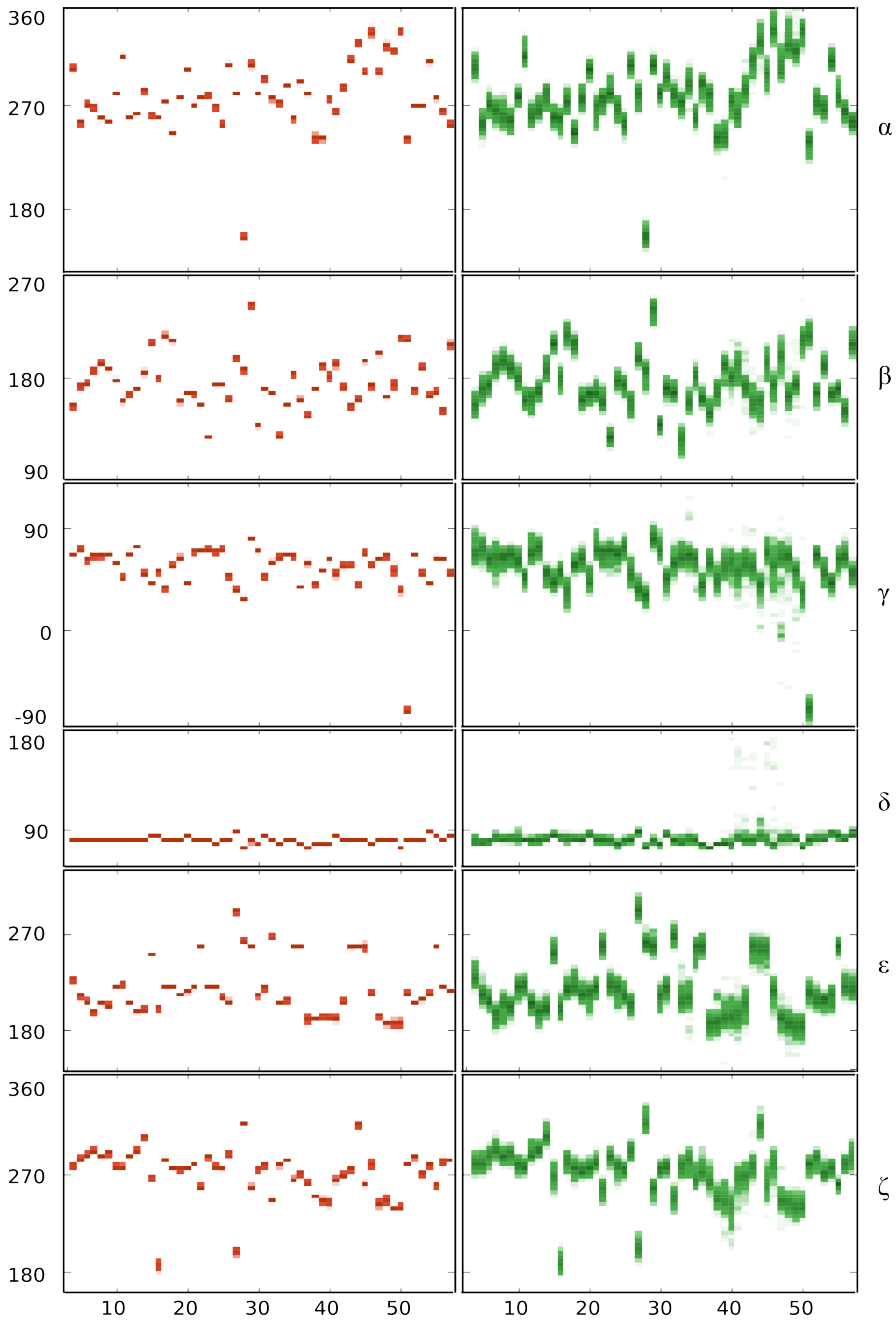


**Fig. S2.** Backbone torsional distributions for 1,000 iMC (left) and 1,000 KGSrna samples (right) of the MLV readthrough pseudoknot (2LC8). A wider range is sampled with KGSrna as the number of populated 3.6° bins show.

## C Video files

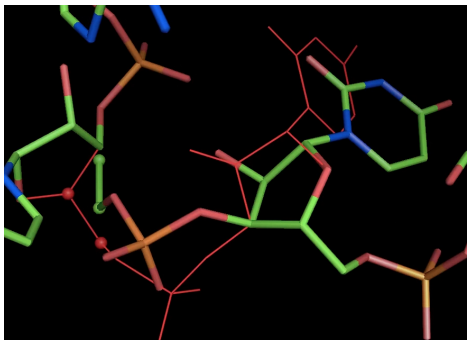

**Fig. S3.** Animation showing the effect on a single nucleotide of running a rebuild perturbation. The ribose conformation has been resampled and a chain-break is introduced on the left side. The animation shows the steps as the chain is reclosed. Video available as supplementary material.

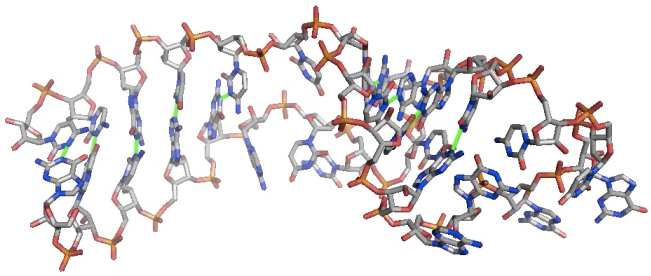

**Fig. S4.** Animation showing the effect on the full chain of running 100 small null space perturbations on the HIV1-TAR RNA molecule. Constraints, highlighted as green bonds, are implicitly maintained through the exact kinematics in KGSrna. Video available as supplementary material.